SANDIA REPORT

SAND97–2631 • UC–704
Unlimited Release
Printed November 1997

Viscosities of Epoxy Encapsulants

Douglas Adolf, Roger Strommen, Harry Johnson

Prepared by
Sandia National Laboratories
Albuquerque, New Mexico 87185 and Livermore, California 94550

Sandia is a multiprogram laboratory operated by Sandia Corporation, a Lockheed Martin Company, for the United States Department of Energy under Contract DE-AC04-94AL85000.

Approved for public release; further dissemination unlimited.

Sandia National Laboratories

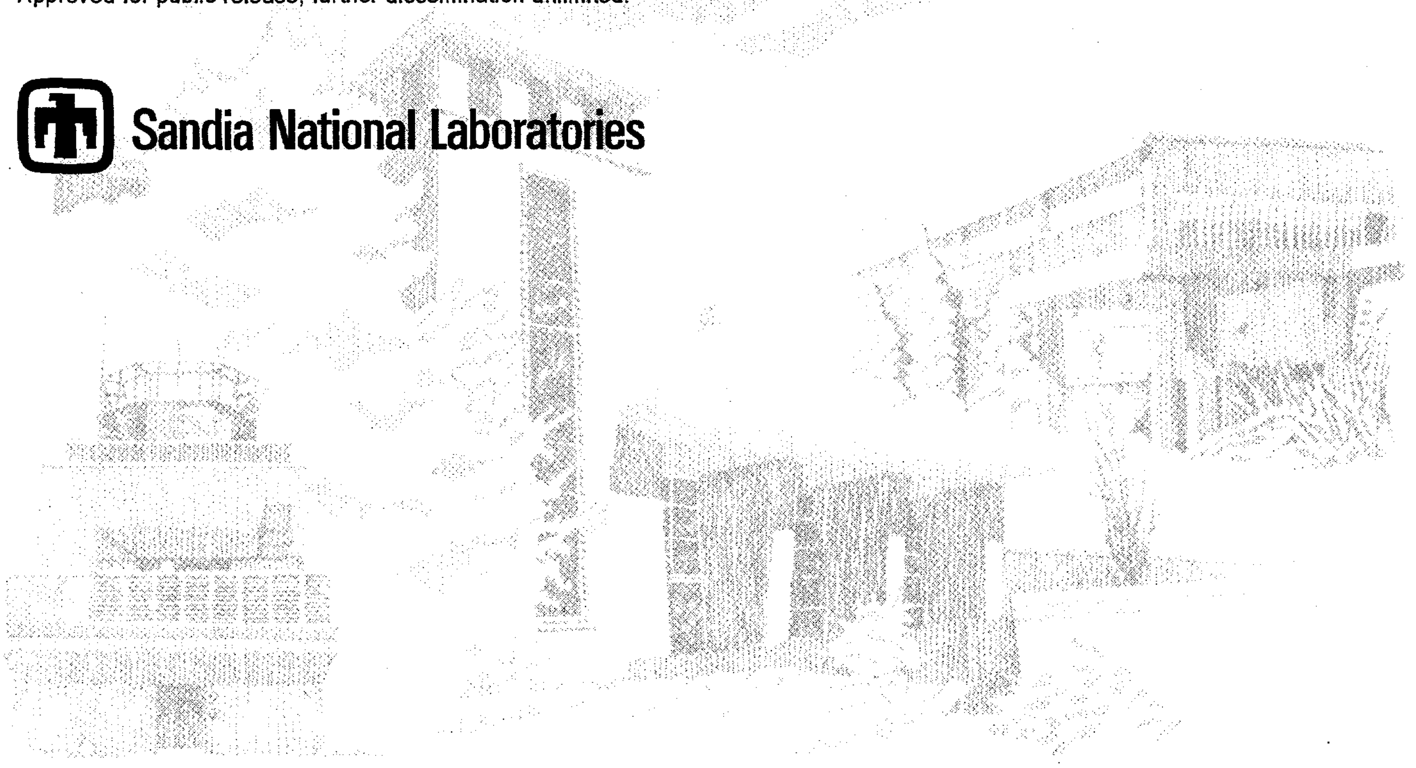

Issued by Sandia National Laboratories, operated for the United States Department of Energy by Sandia Corporation.

Available to DOE and DOE contractors from
Office of Scientific and Technical Information
P.O. Box 62
Oak Ridge, TN 37831

Prices available from (615) 576-8401, FTS 626-8401

Available to the public from
National Technical Information Service
U.S. Department of Commerce
5285 Port Royal Rd
Springfield, VA 22161

NTIS price codes
Printed copy: A03
Microfiche copy: A01

Distribution Category UC-704

SAND 97-2631
Unlimited Release
Printed November 1997

Viscosities of Epoxy Encapsulants

Douglas Adolf, Roger Strommen, and Harry Johnson
Theoretical and Computational Materials Modelling Department
Sandia National Laboratories
P.O. Box 5800
Albuquerque, NM 87185-0333

Abstract

The temperature, curing, and filler dependencies of the viscosities of common epoxies used at Sandia as encapsulants are presented along with examples of useful applications.

I. Introduction

Whereas much effort has been expended over the years to measure the thermophysical properties of solid epoxy encapsulants for stress calculations, little characterization of the liquid epoxies has been attempted. Such characterization could be applied to optimization of processing time/temperature schedules, simulation of mold filling to eliminate void formation, or prediction of filler settling during cure. Moreover, this liquid characterization is non-trivial due to the numerous dependencies we need to investigate. For example, processing typically occurs from temperatures of 65 to 95^{o}C over which the viscosity can change by a factor of 7. More dramatic is the change in viscosity with filler level, where addition of 45 vol.% alumina can increase the viscosity by a factor of 70 and even induce non-Newtonian behavior. Most dramatic, however, is the dependence on state of cure, since at the gel point, the viscosity diverges. In the following report, formalisms are documented that capture these dependencies, and common Sandia epoxies are characterized.

Shell Epon 828, the digylcidyl ether of bisphenol A and the only epoxy resin used in these studies, was cured with either diethanolamine (DEA) or Shell Curing Agent "Z" (a mixture of aromatic amines) and filled with glass microballoons (GMB), tabular alumina (Alox), β-eucryptite (β-eu), or rubber toughener (CTBN). All chemicals and fillers, curing and processing schedules, storage and handling procedures, and stoichiometric ratios followed those detailed in current process specifications. All rheological measurements on unfilled samples were performed with cone-and-plate fixtures while filled sample measurements employed Couette geometry. Parallel or cone-and-plate geometries yielded spurious results in filled systems due to particulate settling or flotation. A Rheometrics RFS-II was used for all testing.

II. Temperature Effects

The temperature dependent viscosities of 828, 828/DEA, 828/Z, and 828/CTBN are shown in Fig. 1 and given in Table 1.

Table 1

temp (C)	828 (P)	828/DEA (P)	828/Z (P)	828/CTBN (P)
20	120			
25	50.0			242
30	22.0	490	50.0	121
35	12.0			65.0
40	6.50	100	11.0	35.0
45	4.00			
50	2.50	23.0	3.40	13.0
55	1.65			
60	1.10	7.00	1.25	6.00
65	0.80			
70	0.60	2.60	0.55	3.00
75	0.44			
80	0.34	1.25	0.26	1.50
85	0.27			

All data can be reduced by the familiar "WLF" equation

$$\log \frac{\eta(T)}{\eta(T_o)} = \frac{-C_1(T - T_o)}{C_2 + T - T_o} \qquad (1)$$

where the required parameters are given in Table 2 below.

Table 2

system	C_1	C_2 (°C)	T_o (°C)	$\eta(T_o)$ (P)
828	3.09	119	70	0.60
828/DEA	4.65	123	70	2.60
828/Z	4.28	127	70	0.55
828/CTBN	4.19	125	70	3.00

Fig. 1: Temperature Dependence of Epoxy Resins

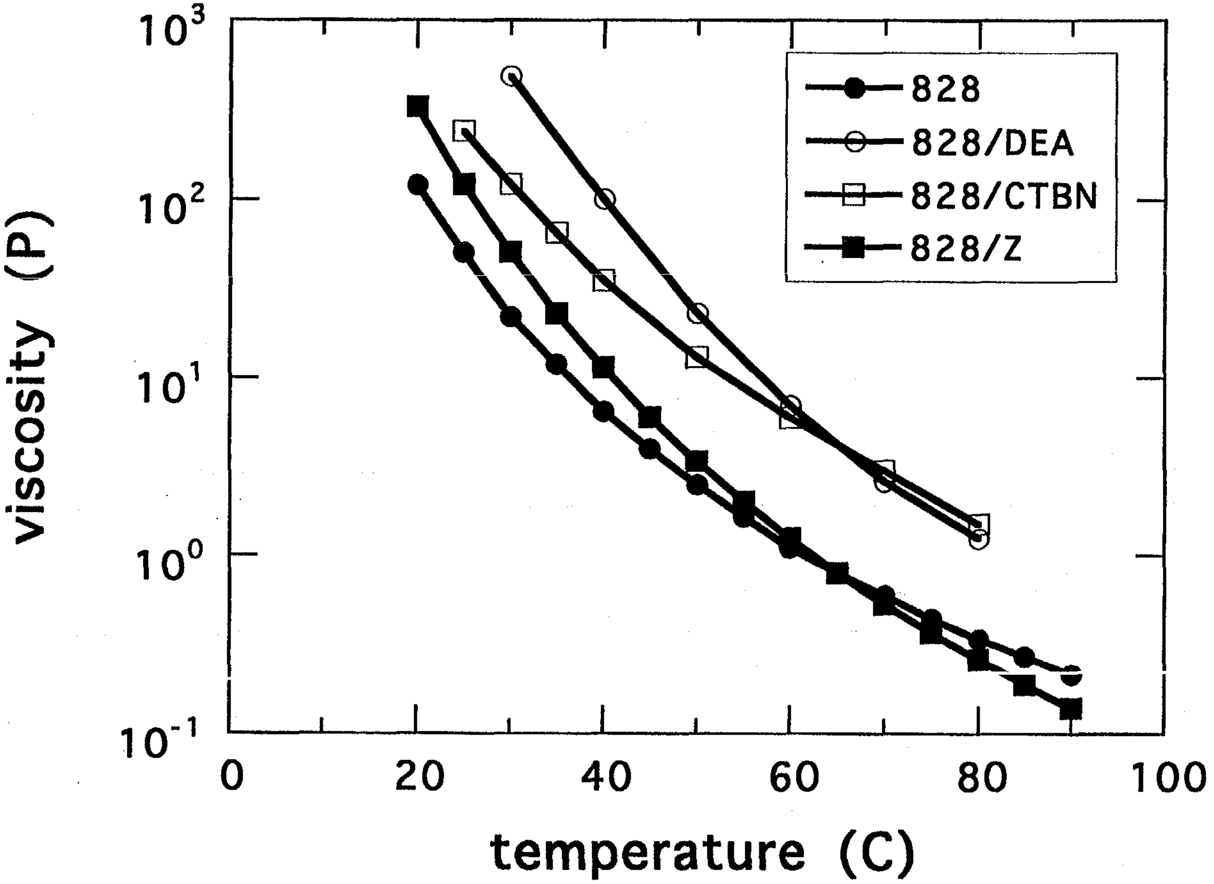

The 828/DEA and 828/Z systems are reactive so the viscosities naturally increase with time. The temperature dependence for Z given here describes the "initial" viscosity immediately after mixing. The situation for 828/DEA is more complicated since the 828 and DEA are actually immiscible immediately after mixing as seen by the cloudy appearance. Only after the reactive DEA amino-hydrogen has endcapped the 828 does the system clear and become homogeneous. We call this preliminary reaction "adduct formation". The temperature dependence given in Table 2 describes the 828/DEA viscosity immediately after adduct formation, but before any true crosslinking reaction takes place.

III. Chemistry Effects

A. DEA adduct formation

Describing the viscosity increase during DEA adduct formation is important since mixing, degassing, and even pouring may be performed during this period. We first must determine the increase in extent of reaction, p, with time for isothermal cures. Fig. 2 shows the adduct reaction rate for isothermal cures at 70, 80, and 90C as measured by differential scanning calorimetry (DSC). These data can be fit moderately well by a rate equation of the form

$$\frac{dp}{dt} = \left(2x10^{9}\ \mathrm{min}^{-1}\right)e^{-(15{,}100\mathrm{cal/mole})/RT}\ p^{0.5}\left(1-p\right)^{1.5} \qquad (2)$$

The heat of reaction was found to be 90 J/g.

Fig. 3 shows the increase in steady shear viscosity during these cures measured independently using cone-and-plate fixtures. And in Fig. 4, the viscosity is crossplotted against the extent of reaction integrated from the DSC data. Even in Fig. 4, we do not see universal behavior since the

Fig. 2: DEA Adduct Formation

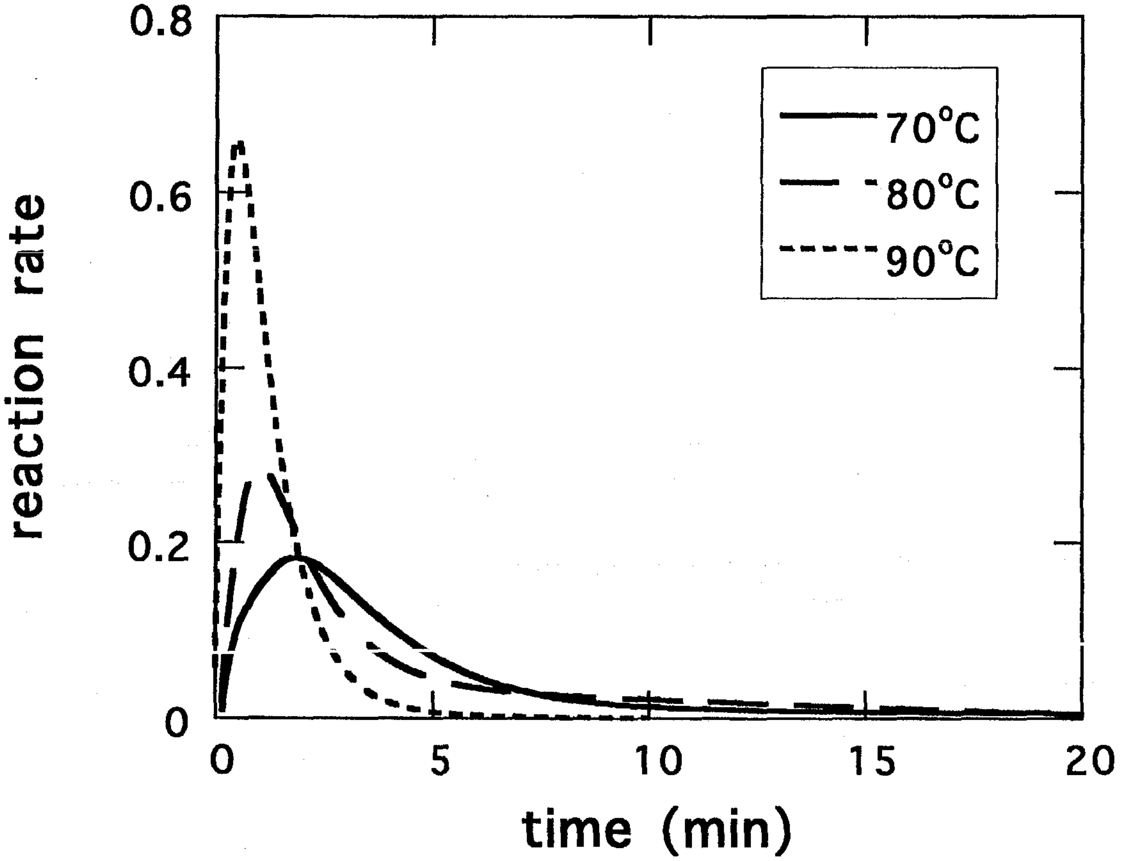

Fig. 3: Viscosity Increase During DEA Adduct Formation

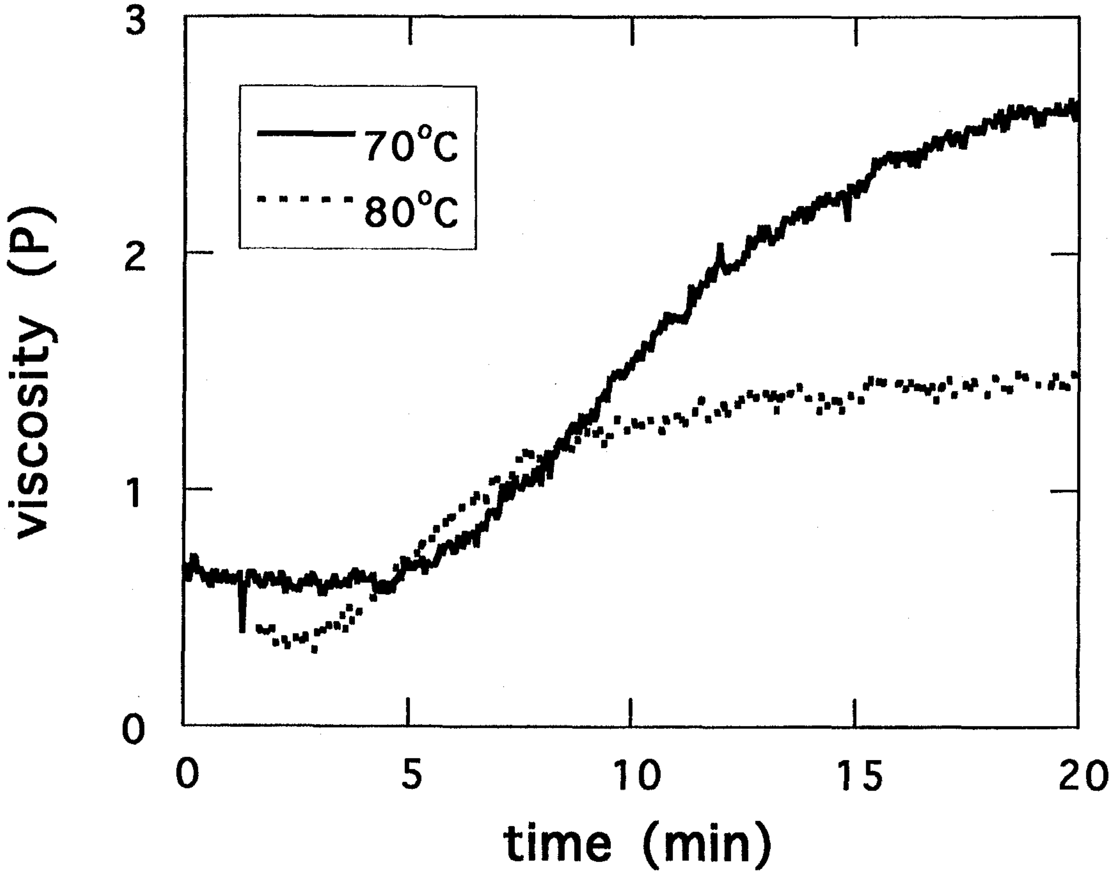

Fig. 4: Viscosity Dependence Upon Extent of Reaction

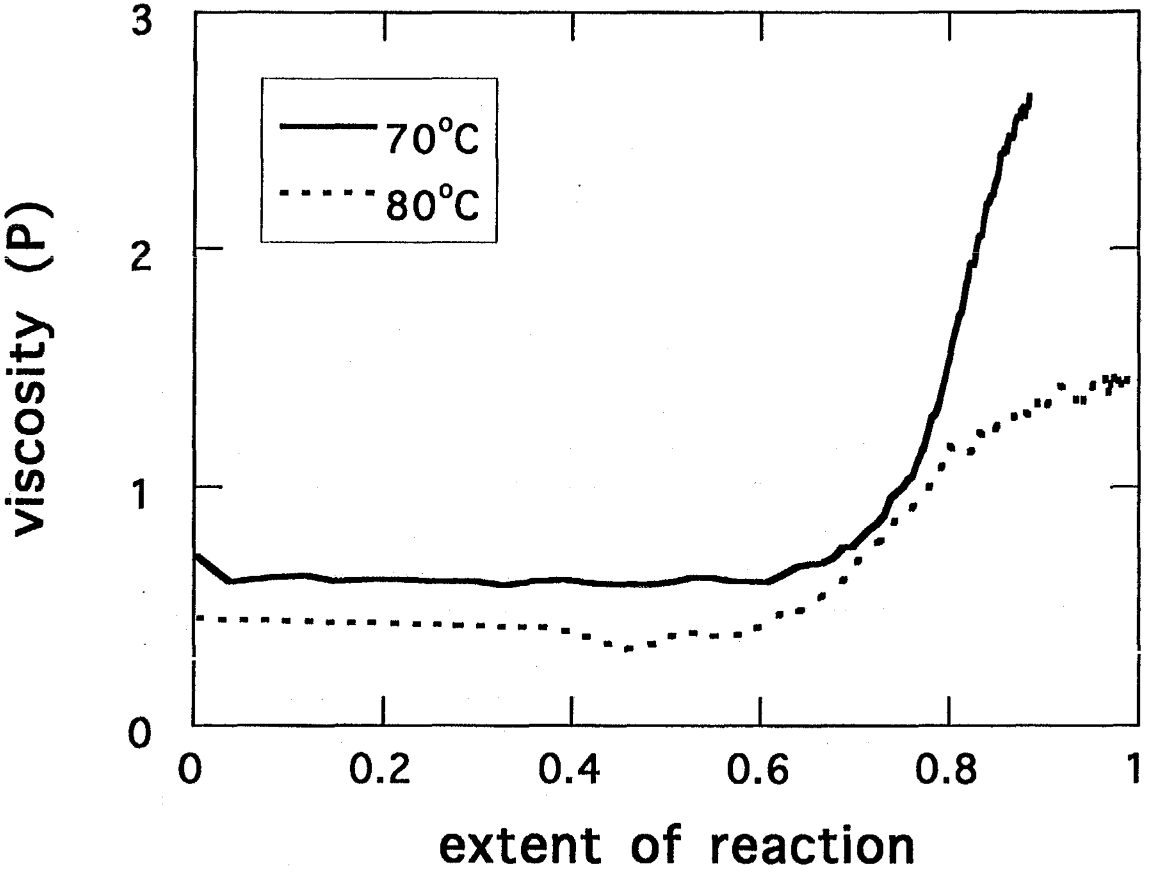

viscosities at the beginning, η_o, and end, η_∞, of adduct formation are temperature dependent. [η_∞, here, would be equivalent to the temperature-dependent 828/DEA viscosity of Table 1.] Therefore, in Fig. 5, we plot the normalized viscosity defined as

$$\frac{\eta - \eta_o}{\eta_\infty - \eta_o} \qquad (3)$$

against the extent of reaction and obtain a fairly universal curve. Note that the viscosity does not rise smoothly with extent of reaction, but appears to increase sharply only after most (~70%) of the adduct reaction has been completed. This almost discontinuous behavior may be due to the fact that the initial reaction bath is actually two-phase and much of the adduct formation may occur at the interface of these phases. If so, this intitial reaction would only tend to enlarge the "DEA balls" which, in turn, would not grossly affect the viscosity. However, near adduct completion, the DEA is chemically solubilized, the reaction bath becomes one-phase, and the viscosity could increase significantly.

B. Gelation

We previously have intensively studied and documented the evolution of viscoelasticity during the crosslinking of these epoxies[1] and so will only briefly review it here. A consistent theoretical framework can be established based on two experimentally validated premises: (1) the evolution of network structure follows percolation predictions and (2) the individual chain dynamics are "Rouse-like" [i.e. behave as a system of beads and springs]. The theory predicts that the viscosity increases as

$$\eta(p,T) = \eta(0, T - T_g)\, \varepsilon^{-4/3} \qquad (4)$$

Fig. 5: Universal Relationship Between Reduced Viscosity and Extent of Reaction

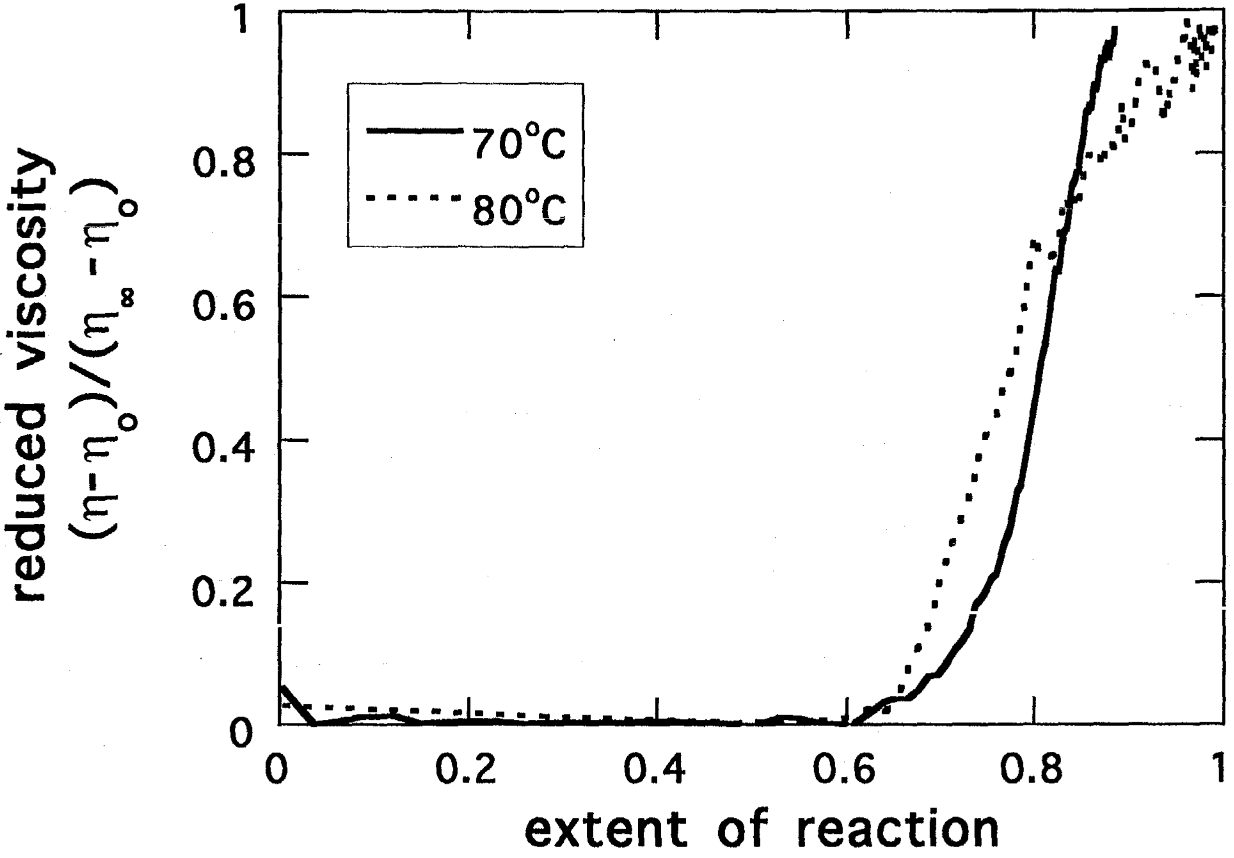

$$\text{where } \varepsilon = \frac{p_g^2 - p^2}{p_g^2} \tag{5}$$

$$\text{and } \log \frac{\eta(0, T - T_g)}{\eta(0,0)} = \frac{-C_1 (T - T_g)}{C_2 + T - T_g} \tag{6}$$

$$\text{with } T_g = \frac{T_g^o}{1 - Ap} \tag{7}$$

It is probably useful, if not necessary, to explain each of the terms in Eq.'s 4-7. $\eta(p,T)$ is the quantity of interest, the epoxy shear viscosity at temperature T and extent of reaction p. The dependence on extent of reaction arises from two factors: (1) the crosslinking reaction increases the average molecular weight of the sol which, in turn, increases the viscosity and (2) the glass transition temperature, T_g, increases with extent of reaction as described by Eq. 7 [T_g^o is the T_g of the unreacted but mixed reactants]. The $\varepsilon^{-4/3}$ term in Eq. 4 captures this first effect. Note that at the gel point, p_g, this term diverges, which is qualitatively correct. However, it is quantitatively correct only at constant $T-T_g$. For example, even the unreacted epoxy would exhibit a divergent viscosity as we cool and it vitrifies. We described this temperature dependence of the unreacted epoxy by Eq. 1. We have experimentally determined that this relationship also holds during cure if we account for the changing T_g. We, therefore, need to modify the $\varepsilon^{-4/3}$ term by the factor $\eta(0,T-T_g)$ in Eq. 6, which gives the temperature dependence of the viscosity as it deviates from the current glass transition temperature. To simplify nomenclature, we choose the WLF reference temperature to be the current T_g. $\eta(0,0)$, then, is the viscosity of the initial reactants at the unreacted glass transition temperature. The constants in Eqs. 4-7 for our epoxies are presented in Table 3

Table 3

epoxy system	p_g	$\eta(0,0)$ (P)	C_1	C_2 (°C)	T_g^o (°K)	A
828/DEA	0.65	1×10^{10}	14.2	40.4	260	0.2
828/Z	0.75	7×10^{7}	12.4	43.8	260	0.25

Tables 3 and 1 predict identical behavior for the unreacted epoxy. Table 1 employs the more convenient reference temperature of 70°C when dealing only with the unreacted epoxies, while Table 3 uses the more convenient current T_g when dealing with arbitrary extent of reaction (-13°C for the unreacted epoxy). The reference temperature affects the values of C_1 and C_2 in the following manner

$$C_2^{\text{new}} = C_2^{\text{old}} + T_{\text{new}} - T_{\text{old}}$$
$$C_1^{\text{new}} = \frac{C_1^{\text{old}} C_2^{\text{old}}}{C_2^{\text{new}}} \qquad (8)$$

which we can use to accord Tables 1 and 3.

Obviously, these equations require a knowledge of the increase in extent of reaction with time. The reaction rates for 828/Z and 828/DEA from 55 to 100C are respectively given by

$$\frac{dp}{dt} = k\left(0.11 + p^{1.2}\right)\left(1-p\right)^{1.35}$$
$$\text{with } \; k = \left(1.2\text{x}10^{6}\ \text{min}^{-1}\right)e^{-(12000\text{cal/mole})/RT} \qquad (9)$$

and

$$
\begin{aligned}
&\frac{dp}{dt} = \left(k_1 + k_2 p^m\right)(1-p)^{1.6} \\
&\text{with } \; k_1 = \left(2.6\text{x}10^7 \text{ min}^{-1}\right)e^{-E/RT} \qquad E = 15.9 \text{ kcal / mole} \\
&\text{and } \quad \text{for } T < 65\text{C} \quad m = 2 \quad \text{and } \; k_2 = \left(5.7\text{x}10^8 \text{ min}^{-1}\right)e^{-E/RT} \\
&\qquad \text{for } 65\text{C} < T < 90\text{C} \quad m = 74\ k_2 \; \text{ where} \\
&\qquad\qquad\qquad k_2 = \left(9\text{x}10^7 \text{ min}^{-1}\right)\left(\frac{90 - T\ (\text{in }^{o}\text{C})}{T\ (\text{in }^{o}\text{C})}\right) \\
&\qquad \text{for } T > 90\text{C} \quad m = k_2 = 0
\end{aligned}
\tag{10}
$$

The complex phenomenological description of the 828/DEA rate in Eq. 9 reflects the equally complex chemical mechanisms of this crosslinking reaction.

IV. Filler Effects

A. Glass microballoons

Since Sandia only uses filled epoxies, the dependence of viscosity upon filler fraction is required. At 70°C, we investigated all commonly used fillers: glass microballoons (GMB), tabular alumina (Alox), β-eucryptite (β-eu), and a rubber (CTBN) toughened version of GMB. In addition, three types of 3M GMB were studied: D32, our current version, with nominal particle diameter of 35 μ and a methacrylatochromic chloride (MCC) antistatic coating; A20 with nominal particle diameter of 60 μ and MCC coating; and H50 with nominal particle diameter of 30μ and a epoxy silane coupling agent coating. A20 and H50 allow us to investigate the effects of particle size and coating independently. Table 4 lists the filler weights used to obtain the various filler volume fractions for all filler systems, based on 100 parts by weight epoxy (density = 1.2 g/cc).

Table4

filler	filler volume fraction	filler density (g/cc)	weight parts of filler
D32	0.30	0.32	11
D32	0.40	0.32	18
D32	0.48	0.32	25
D32	0.55	0.32	33
D32	0.60	0.32	40
A20	0.48	0.20	15
H50	0.48	0.50	38
Alox	0.37	3.98	200
Alox	0.43	3.98	250
Alox	0.48	3.98	300
β-eu	0.37	2.37	115
β-eu	0.43	2.37	150
β-eu	0.48	2.37	185
CTBN/D32	0.30	0.32	11
CTBN/D32	0.40	0.32	18
CTBN/D32	0.48	0.32	25

The D32 GMB exhibited no intrinsic time dependence, as seen by a sharp rise to a steady state viscosity in response to a constant shear rate and by reversible behavior in response to increasing or decreasing shear rate ramps. Additionally, D32 exhibited almost Newtonian behavior with only a hint of shear-thickening at 48 vol.%, as seen in Fig. 6. Fig. 7 shows that A20 and H50 are slightly more viscous and shear-thickening at 48 vol.%. We originally thought that H50, with its epoxy coating might be less viscous and easier to process, but no such luck. It actually showed the highest viscosity.

Fig. 6: Shear Rate Dependence of GMB-Filled 828

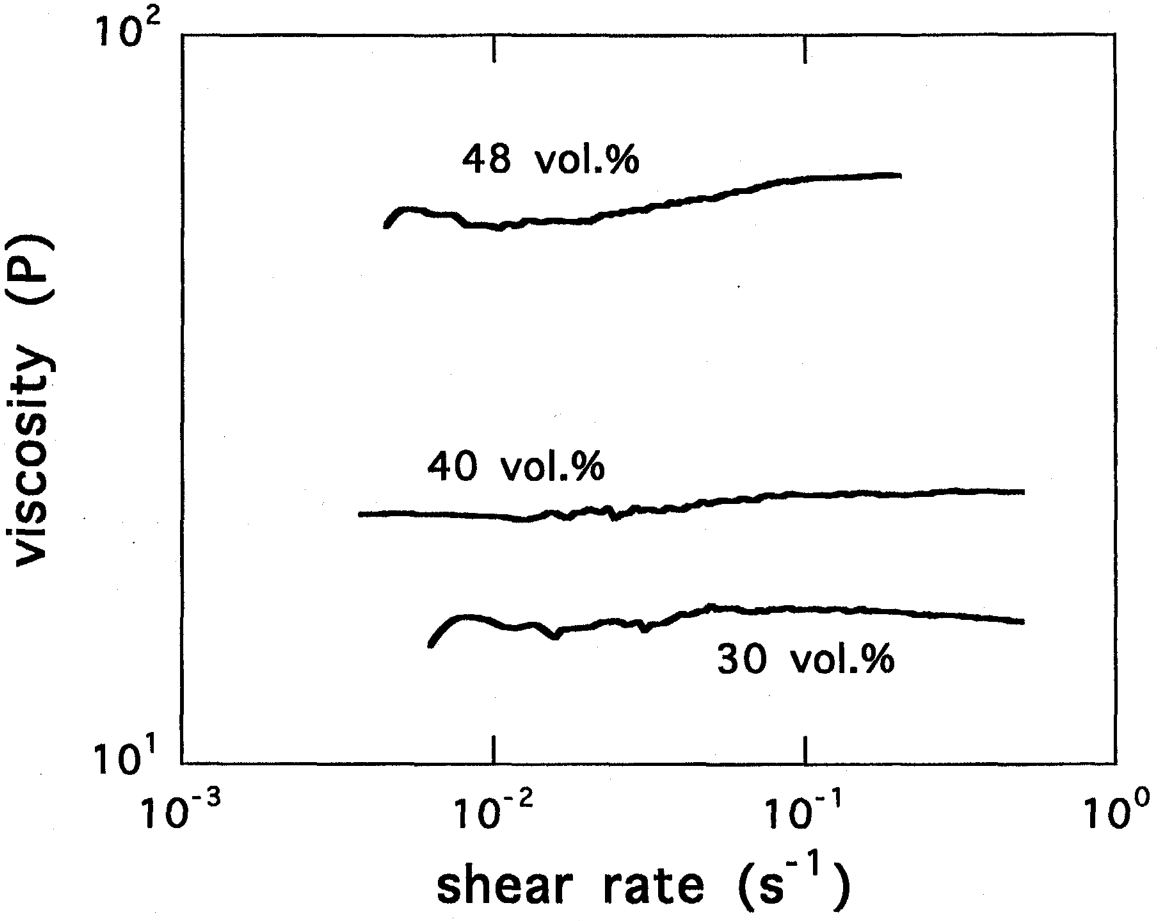

Fig. 7: Various GMB's at 48 vol.% in 828

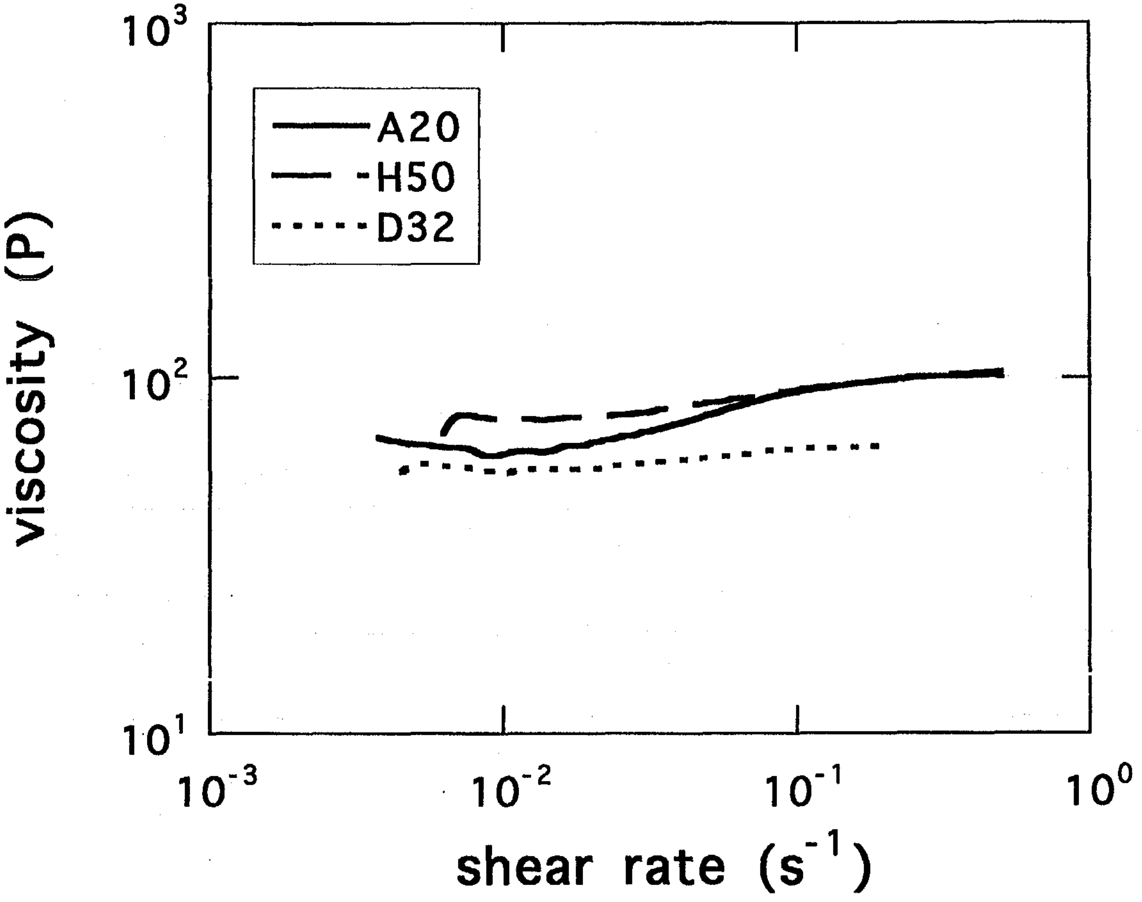

B. Alumina and β-Eucryptite

Alox exhibited definite time and shear rate dependencies. In Fig. 8, we show the approach to steady state in response to constant shear rates for a 48 vol.% suspension. In Fig. 9, we plot the steady state viscosity and time to achieve this value as a function of shear rate for the three different Alox volume fractions. The time to reach steady state is roughly inversely-proportional to the shear rate, $\tau \sim \dot{\gamma}^{-1}$, and the steady state viscosity is definitely shear thickening. That Alox is so different from GMB is not surprising since tabular alumina is a very polydisperse blend of irregular plate-like particles. GMB, by contrast, are extremely smooth spheres and much more mondisperse (particles can still vary easily by a factor of two in radius). From Fig. 9, we can attempt to estimate limiting viscosities at both low and high shear rates. In Fig. 10, we see that these two values are quite distinct. Our typical processing rates, of course, lie somewhere in the transition zone.

Also disturbing is the lot-to-lot variation in Alox viscosities. These are shown in Fig. 11 where we can observe a factor of two difference in the worst case. Previous investigations have attributed these variations to either moisture or particle size. For whatever reason, a difference of two can make these highly filled suspensions unprocessable.

In Fig. 12, we see similar behavior from the β-eu filler. It is perhaps easier to estimate the low shear rate limiting viscosities, but impossible to estimate the high rate limits. The β-eu density of 2.37 g/cc was obtained by helium pycnometry,[2] and electron microscopy[3] clearly shows that the particulates are even more plate-like than Alox, perhaps leading to the more pronounced shear-thickening behavior.

C. Rubber Toughener and General Filler Trends

In Fig. 13, we show all the dependencies of viscosity on filler volume fraction at 70°C in the low shear rate [Newtonian] limit, including that for

Fig. 8: 48 vol.% Alox in 828 at 70°C

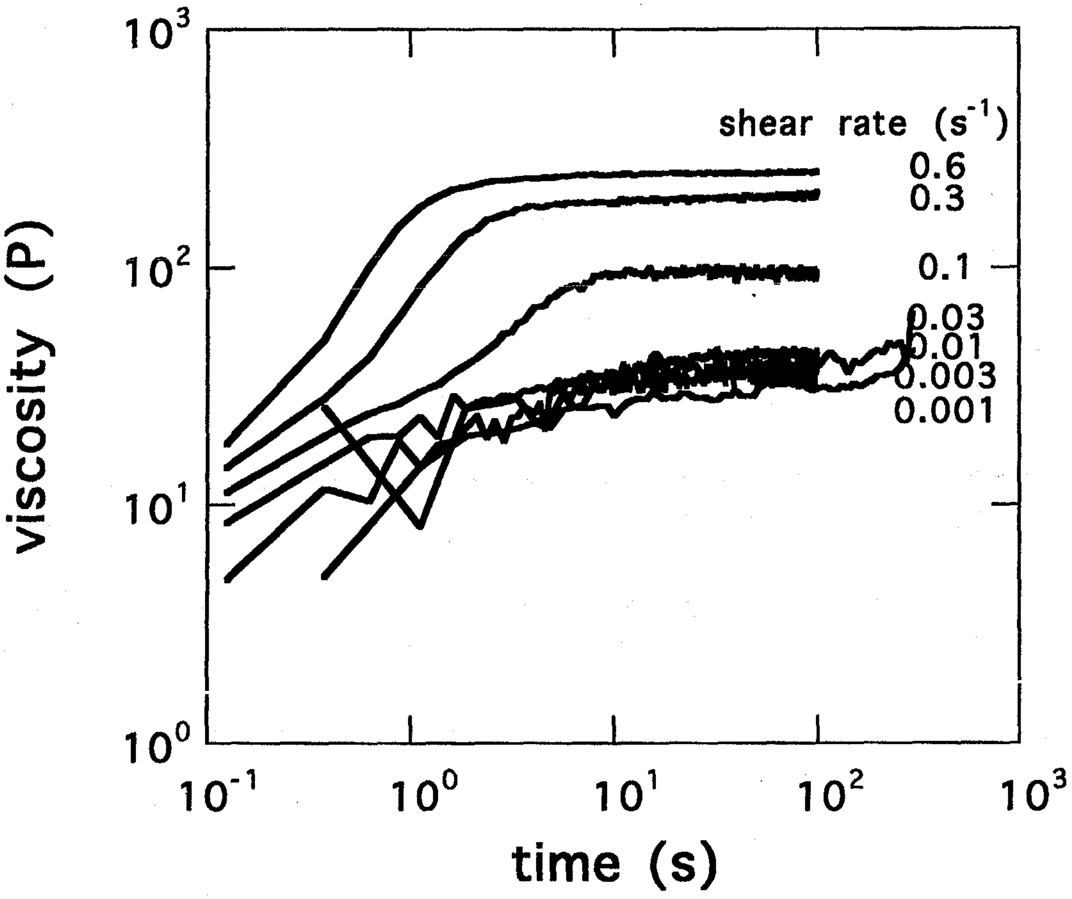

Fig. 9: 828/Alox

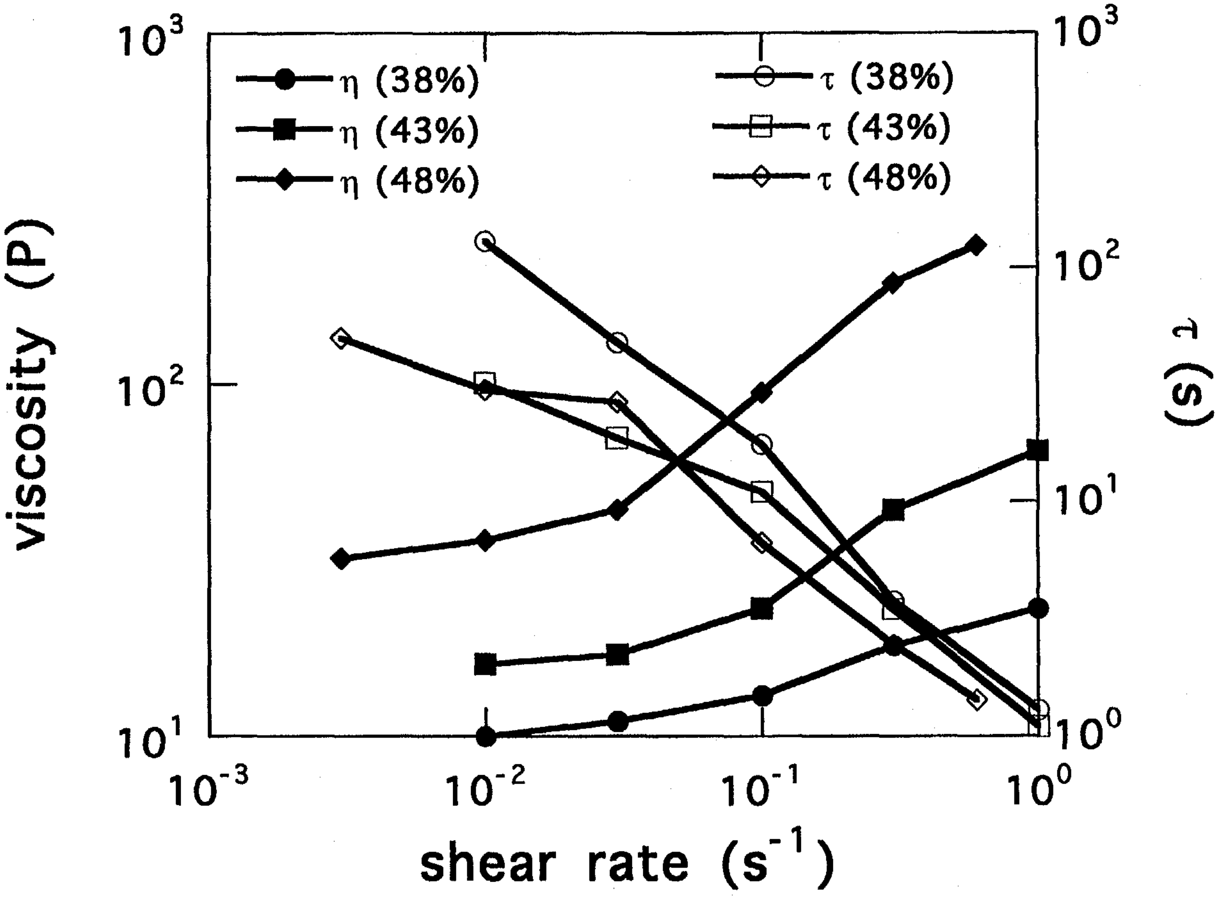

Fig. 10: Limiting Viscosities of 828/Alox at 70°C

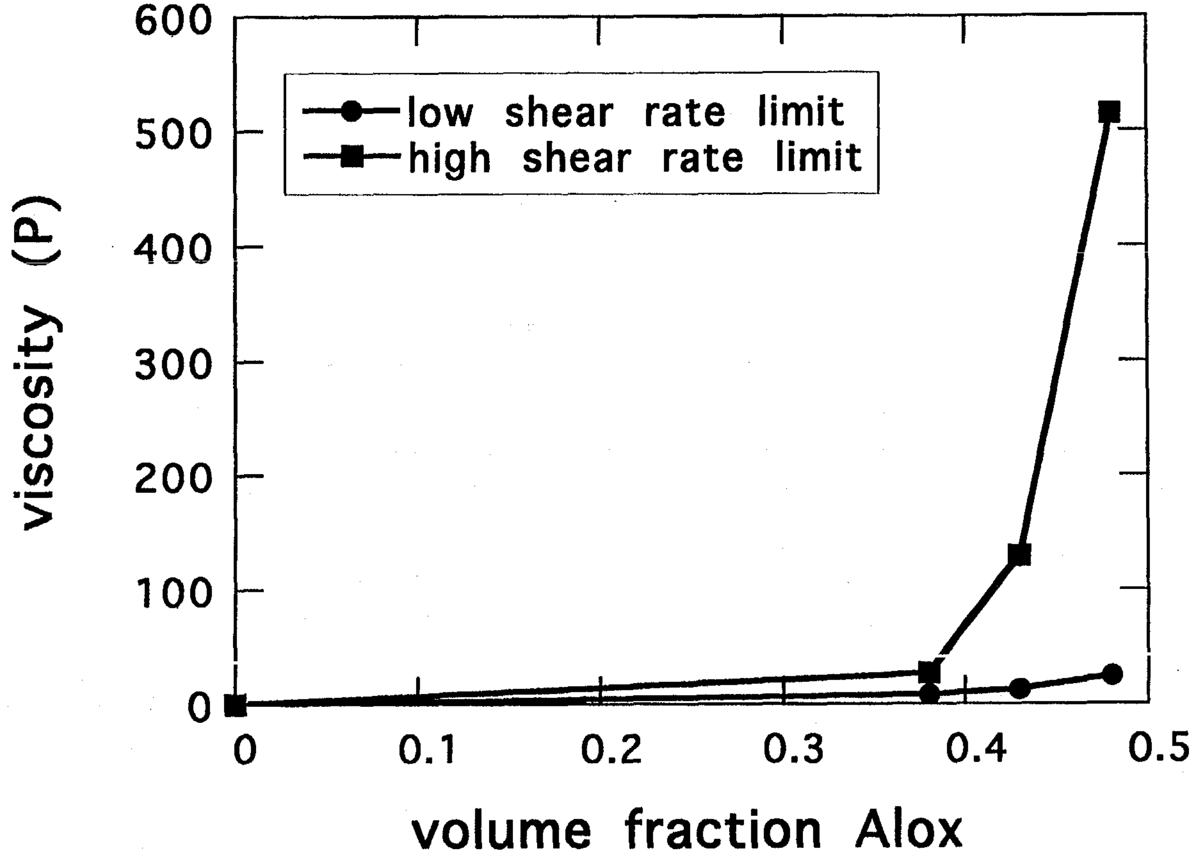

Fig. 11: Various Lots of Alox (48 vol.% at 78°C)

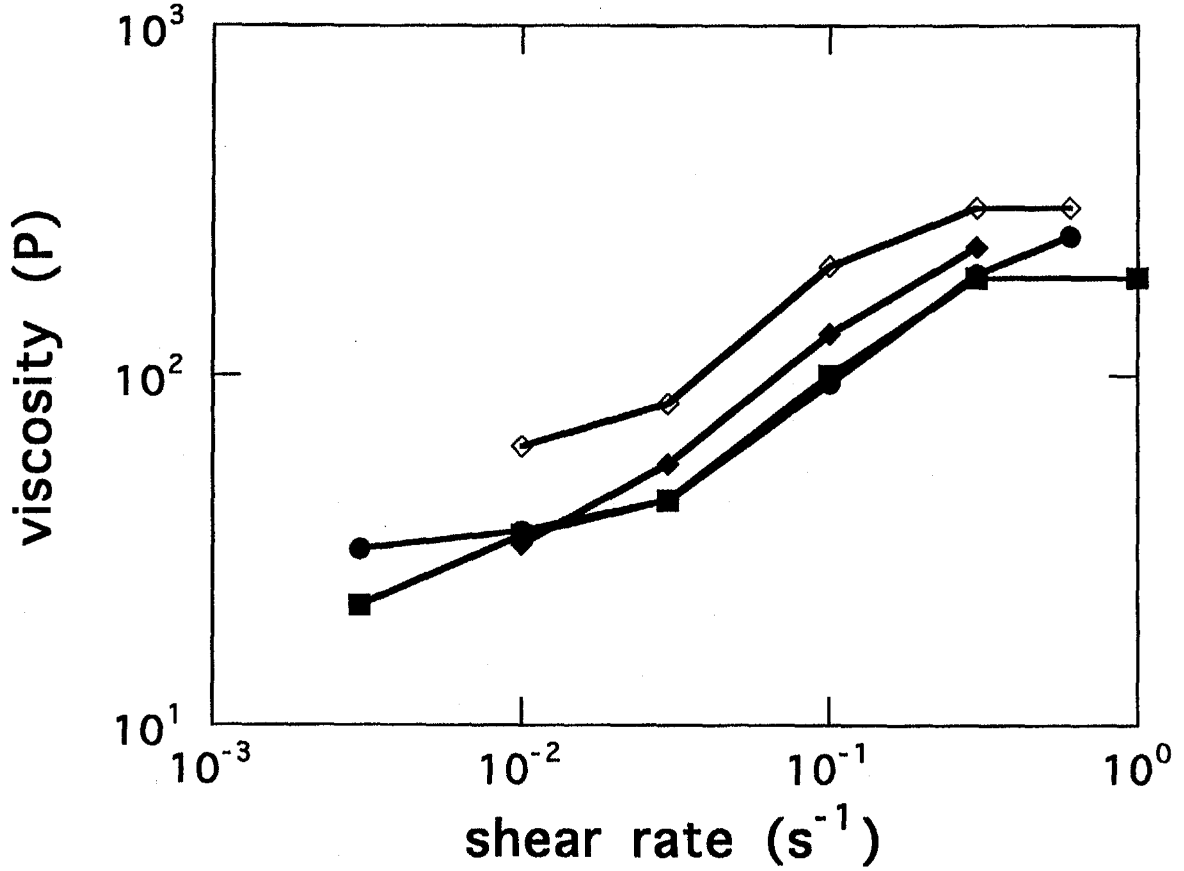

Fig. 12: 828/β-eu at 70°C

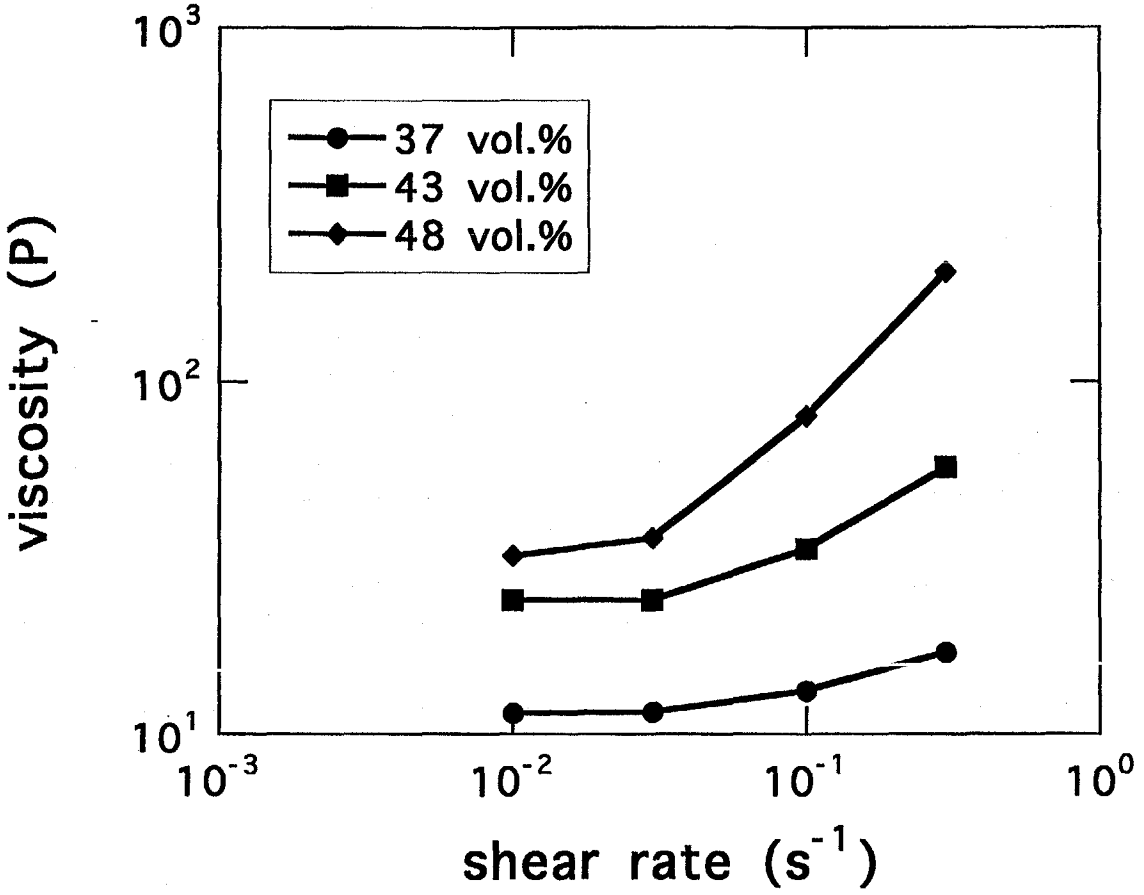

Fig. 13: Comparison of Various Fillers at 70°C

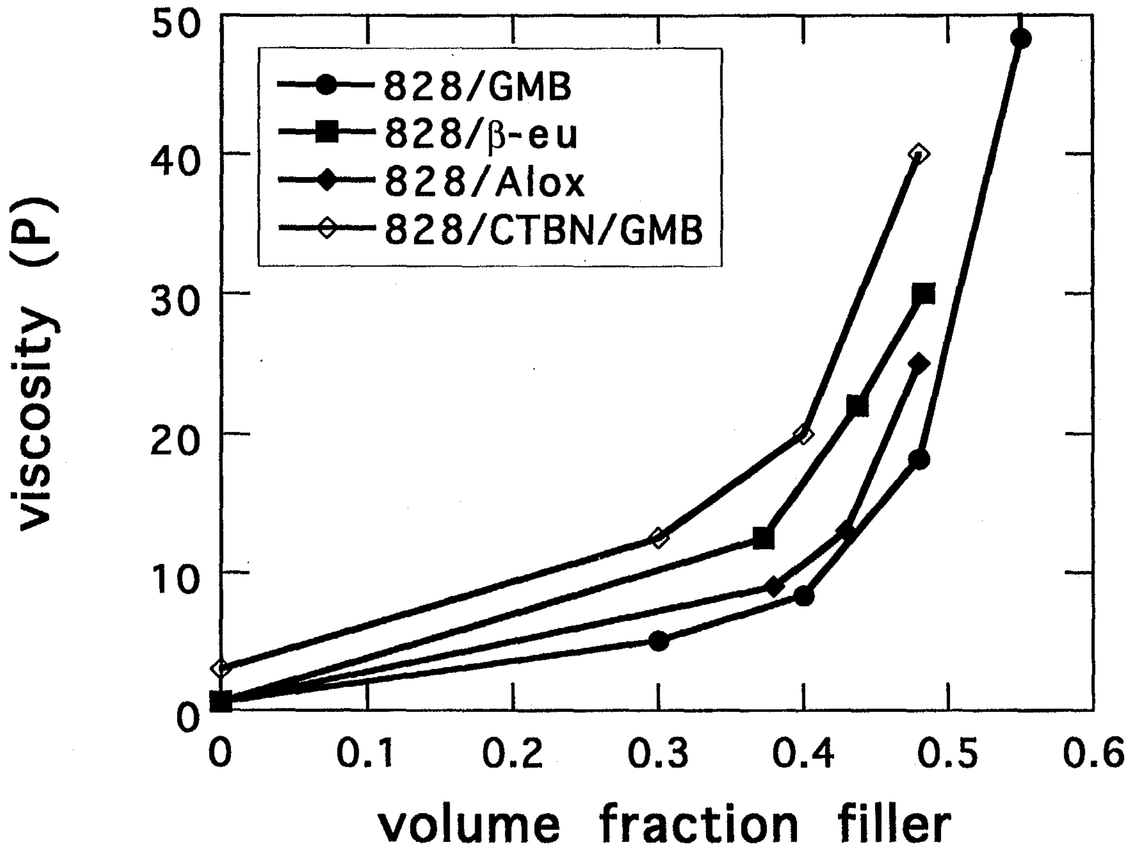

828/CTBN filled with D32 GMB. The trends are not surprising: (1) all viscosities increase sharply with loading levels at volume fractions around 40% and (2) the 828/CTBN filled resin exhibits the highest viscosity [from Table 1, 828/CTBN is 5 times more viscous than 828 alone at 70°C] followed by 828 with plate-like fillers, β-eu and Alox.

The same data are replotted in Fig. 14. The ordinate, now plotted logarithmically, is the reduced viscosity, the measured viscosity normalized by the resin [828 or 828/CTBN] viscosity. Interestingly, the 828/CTBN/GMB system, while exhibiting the highest actual viscosity, shows the weakest dependence on filler volume fraction, and is quite distinct from 828/GMB. The source of this difference is mysterious. Not as mysterious is the observed stronger dependence of the viscosity for the plate-like fillers on volume fraction.

V. Applications

A. Mixing/ degassing/pouring during DEA adduct formation

We will now step through two examples that show how the above data can be used to aid production. In the first example, we will examine the mixing/degassing/pouring of 828/DEA/GMB. By mixing, we mean the addition and stirring of the DEA to the 828/GMB suspension, which implies we will be following the viscosity rise during DEA adduct formation. In current processing schedules, the temperature during degassing is not controlled and is free to rise due to reaction exotherm. Moreover, pouring is begun after the peak exotherm (~100°C) and can continue until the pot cools to below 70°C. One wonders if processing ease and reproducibility could be improved if pouring is postponed until adduct formation is complete, before significant gelation proceeds, and at a controlled temperature which yields a lower viscosity than observed at 70°C under current processing.[4]

Fig. 14: Comparison of Various Fillers at 70°C

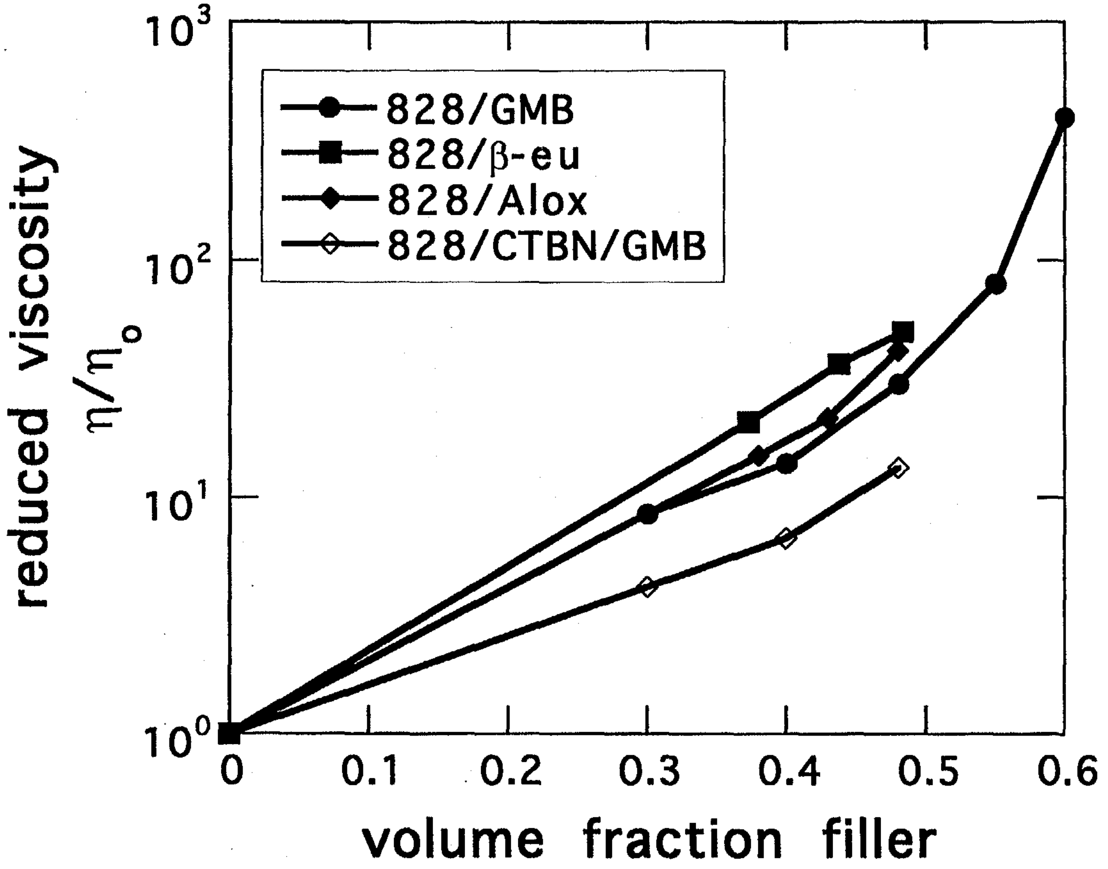

Since our processing window of interest is roughly 20 minutes, Fig. 3 implies that we need only consider the viscosity increase due to adduct formation. The calculations for the viscosity of the current process proceed as follows: (1) prescribe the processing temperature history [this history, in principle, could be calculated with thermal finite element codes using our knowledge of chemical kinetics, heat of reaction, mixing vessel dimensions, and thermal boundary conditions, but for these calculations, we simply assumed a reasonable profile], (2) calculate the adduct formation extent of reaction using Eq. 2, (3) find the reduced viscosity at this extent of reaction from Fig. 5, (4) use Eq. 1 to calculate the actual viscosity at the current temperature [η_∞ corresponds to the 828/DEA viscosity of Table 1 while η_o corresponds to the viscosity of 828 alone], and (5) increase the viscosity by the GMB volume fraction enhancement factor found in Fig. 14. [In the following calculations, we actually neglected this last step which simply renormalizes the viscosity, and simply followed the 828/DEA viscosity rise.]

Fig. 15 shows the increase in viscosity of 828/DEA during adduct formation under the current processing schedule for which the processing temperature reaches a maximum of 100°C. At 17.5 minutes at which the temperature is 70°C, the viscosity is 2.25 P. From Fig. 3, we see that the adduct reaction is almost complete, and from Table 1, we see that the viscosity at adduct completion for 70°C equals 2.6 P. The predicted value of 2.25 P seems reasonable. Again from Table 1, we see that the viscosity at 80°C for complete adduct formation [~15 minutes from Fig. 3] equals 1.25 P. Therefore, we conclude that it might be advantageous to postpone pouring for 20 minutes after adding DEA but pour at a controlled temperature of 80°C. This new schedule has the apparent advantages of improved flow [reduced viscosity] and enhanced reproducibility [pouring occurs after exotherm under a controlled temperature].

Fig. 15: Viscosity Increase During Current Process

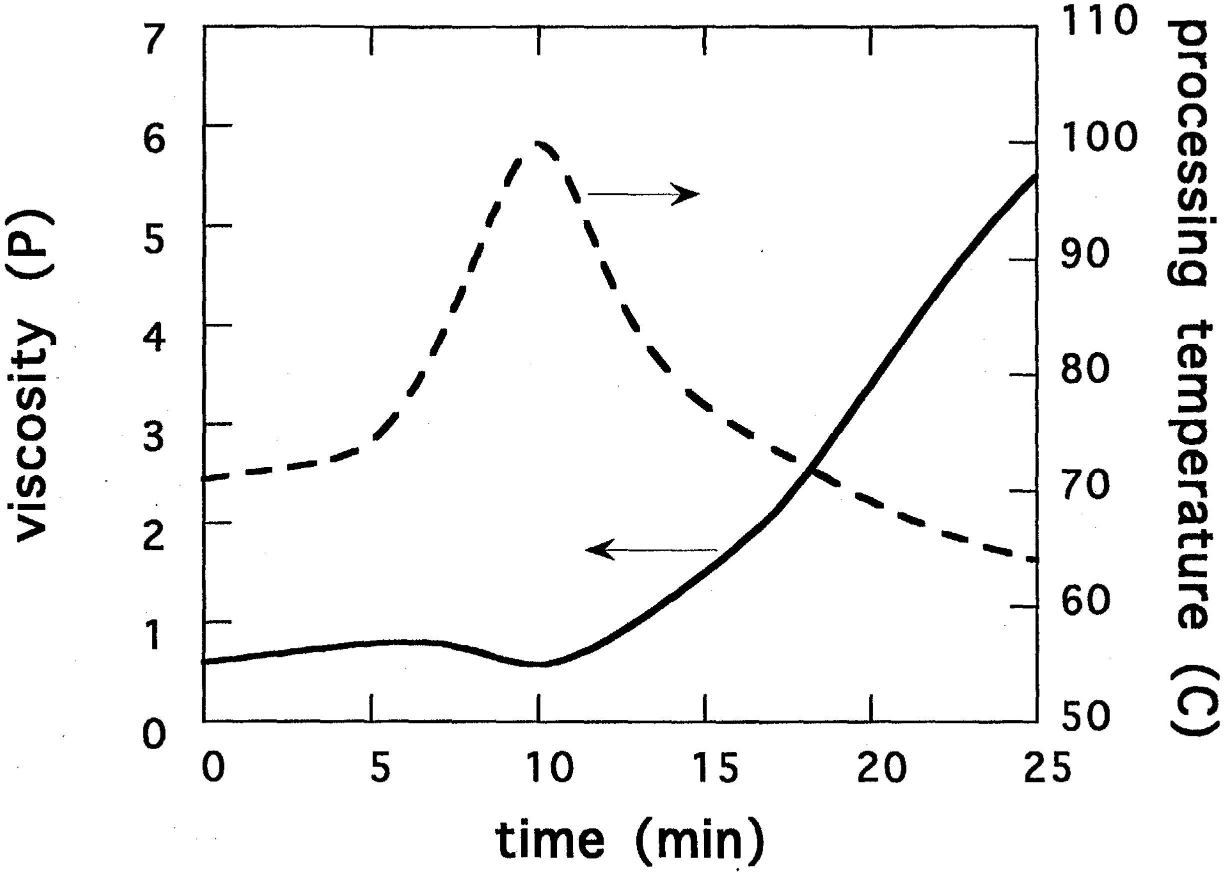

B. 459 potlife

Curing agent "Z", a mixture of aromatic amines, is carcinogenic. The current replacement, "459", employs a mixture of aliphatic amines. It cures somewhat faster than Z, however, which increases the viscosity faster under the standard processing schedule (nominally, a 71°C isothermal cure) and results in reduced "pot life". In this second example, then, we wish to find an isothermal processing schedule for 459 which yields a potlife similar to Z. We will operationally define potlife by the viscosity attained by Z in one hour at 71°C and will, therefore, determine at which temperature does 459 attain this same viscosity in roughly one hour.

In Fig. 16, we show the increase in viscosity of 828/Z as it cures at 71°C over an hour. We first used Eq. 9 to calculate the extent of reaction as a function of time, and then, from Eqs. 4-7, calculated the viscosity increase. The same procedure was used for 459 with

$$\frac{dp}{dt} = k(0.367 + p)(1 - p)^{1.5} \qquad \text{with } k = \left(1.9\text{x}10^{6}\ \text{min}^{-1}\right)e^{-(12000\text{cal/mole})/RT} \tag{11}$$

and

p_g	$\eta(0,0)$ (P)	C_1	C_2 (°C)	T_g^o (°K)	A
0.865	$1.5\text{x}10^7$	12.4	43.8	260	0.29

Fig. 16 also shows the 459 viscosity increase under isothermal cures at 71, 63, and 54°C. At 54°C, the reaction is sufficiently slowed that pot life is similar to 828/Z. Production scale tests confirm these calculations.

Fig. 16: Isothermal Processing Schemes for 828/Z and 459

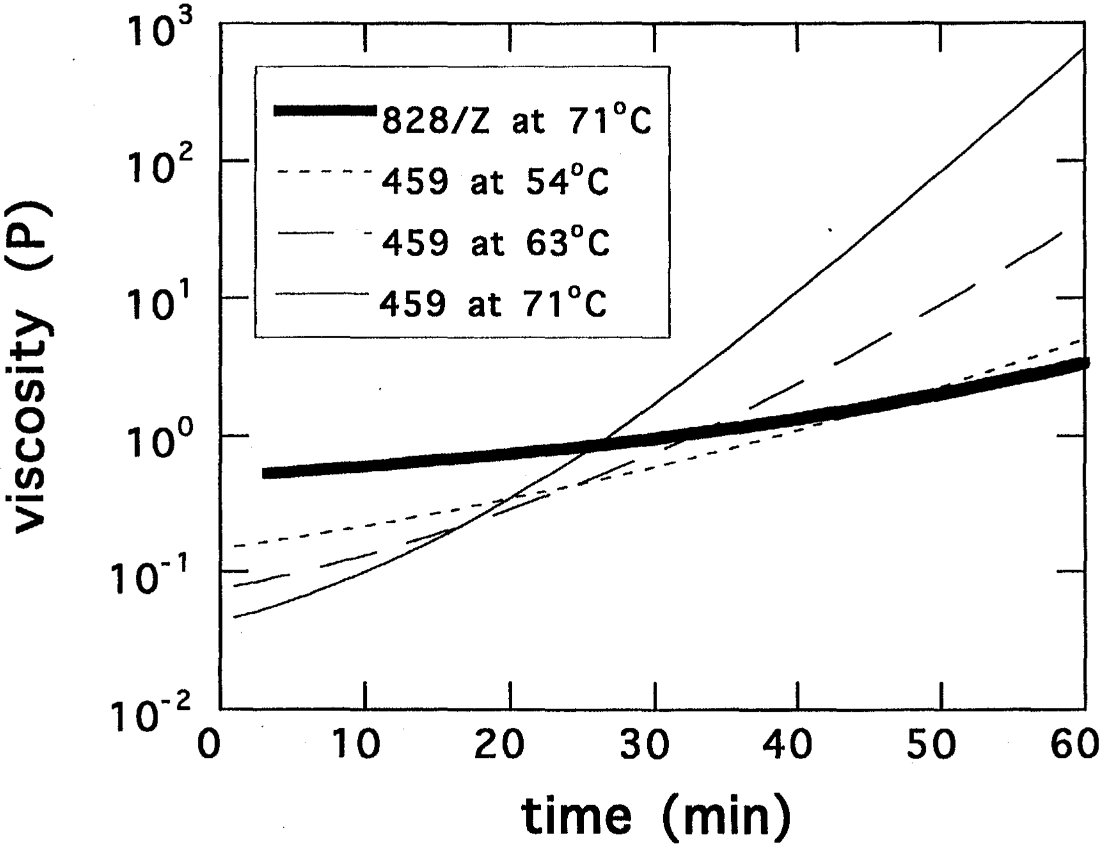

VI. References and Acknowledgements

(1) D. Adolf and J. E. Martin, "Evolution of Structure and Viscoelasticity in Diethanolamine-Cured Epoxy", Sandia Report SAND90-0217, 1990.

(2) Thanks to Bob Lagasse and John Schroeder, 1815.

(3) Thanks to Bonnie McKenzie, 1822.

(4) From Matt Donnelly, 1472.

Distribution

1	MS9018	Central Technical Files, 8940-2
5	0899	Technical Library, 4916
2	0619	Review & Approval Desk, 12690 For DOE/OSTI
10	0333	Doug Adolf, 1841
5	0753	Roger Strommen, 6218
1	0333	Harry Johnson, 1841
1	0961	John Sayre, 1403
1	0958	Carol Adkins, 1472
1	0958	Matt Donnelly, 1472
1	0958	John Emerson, 1472
1	0958	Howard Arris, 1472
1	0958	Mark Stavig, 1472
1	0515	Frank Bacon, 1561
1	0342	Kim Mahin, 1807
1	1407	Bob Lagasse, 1815
1	0343	Mike Keenan, 1824
1	0333	Al Hurd, 1841
1	0328	Marty Stevenson, 2674
1	9404	Linda Domeier, 8713

1	0826	Rehka Rao, 9111
1	0834	Lisa Mondy, 9112
1	0443	Bob Chambers, 9117
1	0443	Steve Burchett, 9117
1	0443	Hal Morgan, 9117
1	0856	Barb Wells, 14482